Evaluation of a Selected Case of the Minimum Dissipative Rate Method for Non-Force-Free Solar Magnetic Field Extrapolations

G. Allen Gary

Center for Space Plasma & Aeronomic Research , The University of Alabama in Huntsville, 320 Sparkman Drive, Huntsville, Alabama 35899 USA

Submitted to Solar Physics

The minimum dissipative rate (MDR) method for deriving a coronal non-force-free magnetic field solution is partially evaluated. These magnetic field solutions employ a combination of three linear (constant-α) force-free-field solutions with one being a potential field (i.e., α=0). We examine the particular case of the solutions where the other two α's are of equal magnitude but of opposite signs. This is motivated by studying the SOLIS[1] vector magnetograms of AR 10987 which show a global α value consistent with an α=0 value as evaluated by $(\nabla\times B)_z/B_z$ over the region. Typical of the current state of the observing technology, there is no definitive twist for input into the general MDR method. This suggests that the special α-case, of two α's with equal magnitudes and opposite signs, is appropriate given the data. Only for an extensively twisted active region does a dominant, non-zero α normally emerge from a distribution of local values. For a special set of conditions, we find: (i) The resulting magnetic field is a vertically inflated magnetic field resulting from the electric currents being parallel to the photosphere, similar to the results of Gary and Alexander (1999). (ii) For $\alpha \sim (\alpha_{max}/2)$, the Lorentz force per unit volume normalized by the square of the magnetic field is on the order of 1.4×10^{-10} cm^{-1}. The Lorentz force (L_F) is a factor of ten higher than that of the magnetic force $d(B^2/8\pi)/dz$, a component of L_F. The calculated photospheric electric current densities are an order smaller than the maximum observed in all active regions. Hence both the Lorentz force density and the generated electric current density seem to be physically consistent with possible solar dynamics. The results imply that the field could be inflated with an over pressure along the neutral line. (iii) However, the implementation of this or any other extrapolation method using the electric current density as a lower boundary condition must be done cautiously, with the current magnetography.

Magnetic Fields, Coronal Extrapolations, Inflated Magnetic Fields, Non-force-free fields

Introduction

Considerable effort has been spent in specifying the dynamics of solar plasmas by employing conservation laws that relate to constraints on the electromagnetic fields and plasma flows; since their solutions lead to a representation of a relaxed state of the plasma. To include non-equilibrium and non-force-free plasmas with helicity injection, the minimum dissipative rate methods have been introduced. The minimum dissipative rate (MDR) method for deriving the coronal magnetic field is based, in part, on the principle that the relaxed state of a plasma has minimum Ohmic dissipation with a constant global helicity; that is, the magnetic energy dissipation is minimized (Bhattacharyya & Janaki 2004; Bhattacharyya et

[1] Synoptic Optical Long-term Investigation of the Sun (SOLIS), a National Solar Observatory facility.

al. 2007; Dasgupta et al. 2008, Hu et al. 2008, Hu & Dasgupta 2008)[2]. Motivated by Hu et al.'s (2008) application of the MDR method to a solar active region, *we examine and evaluate this approach further using a special subset of solutions in order to determine the magnitude of the resulting forces and their feasibility for solar magnetic field extrapolation.*

The general resulting MDR equations with non-force-free solutions are extensions of the linear force-free-field equation $\nabla\times\mathbf{B} = \alpha\,\mathbf{B}$, but assume different variational equations (or constraints) as the starting point. The MDR approach for the magnetic field is similar to Chandrasekhar & Woltjer's (1958) approach in which a variational approach is used, given the mean-square current density and the maximum magnetic energy, to obtain the field magnetic field equation $\nabla\times\nabla\times\mathbf{B} = \alpha\,\mathbf{B}$, whose solutions include a wider class of solutions than the constant-α force free solutions. By a variation of the constant global Ohmic dissipation rate given the constraint of a constant relative magnetic helicity, one can derive the restricted MDR magnetic field equation $\nabla\times\nabla\times\nabla\times\mathbf{B} = \alpha\,\mathbf{B}$ (Appendix B). The special case of the general MDR equations which we study is given by $\nabla\times\nabla\times\nabla\times\mathbf{B} = \alpha^2\nabla\times\mathbf{B}$. This is a restricted form of the most general Bhattacharyya et al. (2007) two fluid MRD field equation, derived from an extended variational function. These MDR equations are discussed in the next section. Following that section there is a discussion of a special MDR field solution which results in an inflated magnetic field. We derive several relationships between helicity and magnetic energy. We then examine the consequences of the MDR method as applied to a simple bipolar active region, which motivated in part, this study.

MDR Method

In this section we give a background to the general Bhattacharyya et al. (2007) MDR magnetic field solution stemming from a variational approach. First we will consider the related following single-fluid variational problem which leads to nonlinear non-force-free-field solutions (Dasgupta et al. 1998). Given (i) the Ohmic dissipation rate ($\mathcal{R}$), in terms of a constant electric resistive (η) and the electric current density ($\mathbf{j}$), as $\mathcal{R} = \int_V \eta\,\mathbf{j}^2\,dV$, and given (ii) the relative magnetic helicity[3] ($\mathcal{K}_M$), in terms of the magnetic field ($\mathbf{B}$) and its vector potential (A), as $\mathcal{K}_M = \int_V(\mathbf{A}+\mathbf{A}_p)\cdot(\mathbf{B}-\mathbf{B}_p)\,dV$, the MDR variational of $\delta(\mathcal{K}_M - \varepsilon'\,\mathcal{R})=0$ as function of $\mathbf{B}(x,y,z)$, with ε the Lagrange multiplier, leads to the following MDR Euler-Lagrange equation

$$(\nabla\times\nabla\times\nabla\times\mathbf{B}) = \varepsilon\,\mathbf{B}, \qquad (1)$$

where $\varepsilon = \varepsilon'\,\mu^2/\eta$ (see Appendix B for the derivation). This derivation assumes a single fluid in a closed system and the slightly resistive plasma is relaxed under

[2] For a parallel electric circuit, a simple introductory example of the MDR method is given in Appendix A.

[3] The hypothesis for the constancy of the magnetic helicity is based on the following two concepts. Woltjer's (1958) theorem states: the magnetic helicity $\mathcal{K}_M = \int_V \mathbf{A}\cdot\mathbf{B}\,dV$ is an invariant for a perfectly conducting measure in a closed volume. For a plasma where the characteristic diffusion time (τ_d) is much larger than the plasma velocity time scale ($\tau_d = L/vv$), $R_M = \tau_d/\tau_v$, magnetic helicity is approximately conserved (Taylor 1974; Golub & Pasachoff 1997, p. 223) .

the constraint of constant helicity and minimum Ohmic dissipation. The nonlinear non-force-free field solution of Equation (1) can be constructed by a superposition of three linear force-free field solutions (Dasgupta et al. 2008). The more general magnetic field equation derived by Bhattacharyya et al. (2007) assumes a two-fluid resistive plasma with constant helicity injection that balances the helicity dissipation. Following Hu and Dasgupta (2008), the resulting field equation can be expressed in terms of a triple curl product of the field in the form:

$$\nabla\times\nabla\times\nabla\times\mathbf{B} + a_1\,\nabla\times\nabla\times\mathbf{B} + b_1\,\nabla\times\mathbf{B} = 0, \qquad (2)$$

with a_1 and b_1 system constants involving the plasma description and the Lagrange multiplier (Hu et al. 2008). Again as with Equation (1), the solution of Equation (2) is a superposition of force-free field solutions given by

$$\mathbf{B}(x,y,z) = (\omega_1 \mathbf{B_1}(x,y,z) + \omega_2\mathbf{B_2}(x,y,z) + \omega_3 \mathbf{B_3}(x,y,z))/3 \qquad (3)$$

where $\mathbf{B_i}$ satisfies the linear (constant-alpha) force-free field equation,

$$\nabla\times\mathbf{B_i}(x,y,z) = \alpha_i \mathbf{B_i}(x,y,z) \text{ for } i=1,2,3, \qquad (4)$$

where the α_i's are scalar constants(Hu & Dasgupta 2008). The ω_i's are weighting functions which can be formally used to satisfy the vector magnetic field lower boundary conditions, in a global sense (see Hu et al. 2008). For simplicity, in Equation (3) we will assume later an equal weight distribution of the three component fields. A benefit of the solution is that the constant-α fields can be evaluated quickly. In the derivation of Equation (2), Bhattacharyya et al. (2007) assumed a two-fluid plasma, an incompressible flow, a constant helicity dispersion rate, a constant diffusion rate, and a constant thermal diffusion rate. Since the α values are global constants the general solutions of the MDR methods are limited in the sense the solutions can only represent a global average solution. However, given the longitudinal and transverse field at the lower boundary (e.g., photosphere) and allowing the six parameters (three α_i and three ω_i) to be determined by the lower boundary conditions, a minimization of the errors between the observed and the MDR solutions have produced relatively small errors when compared with a nonlinear force-free field extrapolation (Hu et al. 2008).

Inflated Field Solution – A Special Case

We now show (i) that the non-force-free composite solution using the linear-force-free-field solutions, Equation (3), satisfies the Euler-Lagrange magnetic field solution (Equation (2)), (ii) that a_1 and b_1 can be easily evaluated, and (iii) that the special α-case gives an inflated field solution. By substitution of $\mathbf{B}(x,y,z)$ (Equation (4)), we have

$$\nabla\times\mathbf{B} = (\alpha_1 \omega_1\mathbf{B_1} + \alpha_2\omega_2 \mathbf{B_2} + \alpha_3\omega_3 \mathbf{B_3})/3 , \qquad (5)$$

$$\nabla\times\nabla\times\mathbf{B} = (\alpha_1^2\, \omega_1\mathbf{B_1} + \alpha_2^2\, \omega_2\mathbf{B_2} + \alpha_3^2\omega_3\, \mathbf{B_3})/3 \ , \quad (6)$$

$$\nabla\times\nabla\times\nabla\times\mathbf{B} = (\alpha_1^3\, \omega_1\mathbf{B_1} + \alpha_2^3\, \omega_3\mathbf{B_2} + \alpha_3^3\, \omega_3\mathbf{B_3})/3. \quad (7)$$

The Euler–Lagrange equation becomes,

$$[\alpha_1^3\, \omega_1\mathbf{B_1} + \alpha_2^3\, \omega_2\mathbf{B_2} + \alpha_3^3\, \omega_3\mathbf{B_3}] + a_1\, [\alpha_1^2\, \omega_1\mathbf{B_1} + \alpha_2^2\, \omega_2\mathbf{B_2} + \alpha_3^2\, \omega_3\mathbf{B_3}] + b_1\, [\alpha_1\, \omega_1\mathbf{B_1} + \alpha_2\, \omega_2\mathbf{B_2} + \alpha_3\, \omega_3\mathbf{B_3}] = 0, \quad (8)$$

and since $\mathbf{B}_i$ are independent functions, we have the following three equations,

$$\alpha_1^3 + a_1\, \alpha_1^2 + b_1\, \alpha_1 = 0, \quad (9)$$

$$\alpha_2^3 + a_1\, \alpha_2^2 + b_1\, \alpha_2 = 0, \quad (10)$$

$$\alpha_3^3 + a_1\, \alpha_3^2 + b_1\, \alpha_3 = 0. \quad (11)$$

Multiplying Equation (9) by α_3^2 and subtracting from it the product of Equation (10) with α_1^2, the value of b_1 is obtained,

$$b_1 = \alpha_1\alpha_3. \quad (12)$$

Substituting b_1 into Equation (9), we obtain

$$a_1 = -\alpha_1-\alpha_3. \quad (13)$$

Hence the magnetic field equation is

$$\nabla\times\nabla\times\nabla\times\mathbf{B} - (\alpha_1+\alpha_3)\, \nabla\times\nabla\times\mathbf{B} + \alpha_1\alpha_3\, \nabla\times\mathbf{B} = 0, \quad (14)$$

Substitution for a_1 and b_1 into Equation (10), with unequal α values, gives

$$\alpha_2^3 - (\alpha_1+\alpha_3)\alpha_2^2 + (\alpha_1\alpha_{3)}\alpha_2 = 0, \quad (15)$$

which implies that $\alpha_2=0$.

Hu & Dasgupta (2008) considered the specific case of $\alpha_1= -\alpha_3$ and $\alpha_2=0$, which reduces Equation (2) to

$$\nabla\times\nabla\times\nabla\times\mathbf{B} = \alpha^2\nabla\times\mathbf{B}. \quad (16)$$

As they point out, this equation is equivalent to taking an extra curl of the Chandrasekhar-Woltjer result. For this case of $\alpha_1= -\alpha_3$ with equal weighting (i.e., $\omega_1=\omega_2=\omega_3$), there is no dominant twist to the field lines, however the field is inflated as compared to the potential field. The inflation aspect can be seen from the fact that the j_z components are null ($j_z=0$), so that all the electric currents are parallel to the photospheric surface, which cause the field to inflate. With equal weighting functions, this is seen from Equation (5) where we have for the normal z-components,

$$j_z = (\nabla\times\mathbf{B})_z = \alpha_1\, (\mathbf{B_1})_z - \alpha_1\, (\mathbf{B_3})_z \equiv 0. \quad (17)$$

The identity holds since the normal z-components of the field is the same for either $\alpha_1$or $-\alpha_1$. From Gary (1989), for field of finite energy, the z-component of linear FFF solution can be written as

$$B_z(x,y,z) = \iint\, [\, \iint B_z(x',y',z=0)\, e^{-2\pi iux' - 2\pi ivy'}\, dx'dy'] \, e^{-kz + 2\pi iux - 2\pi ivy}\, du\, dv, \quad (18)$$

where $k^2= 4\pi^2(u^2+v^2)-\alpha^2$, and the solution is independent of the sign of α. It is assumed that the photospheric boundary condition is such that the Fourier transform for $B_z(x',y',z=0)$ vanishes for the frequency domain $(u^2+v^2)<\alpha^2$.

Magnetic Energy and Helicity

In this section we derive closed expressions for magnetic energy and the magnetic helicity, and interrelate these quantities. First, however, we relate the global linear force-free parameter α_G to the individual α_i's of Equation (4). Following from the last paragraph, all z-components of the $\mathbf{B_i}$ field are equal, $((\mathbf{B}_1(z=0))_z = (\mathbf{B}_2(z=0))_z = (\mathbf{B}_3(z=0))_z)$, at the photosphere (z=0). Hence

$$\alpha_G=(\nabla\times\mathbf{B})_z/\mathbf{B}_z =(\alpha_1 \mathbf{B_1} + \alpha_2 \mathbf{B_2}+ \alpha_3 \mathbf{B_3})_z/ (\mathbf{B_1} + \mathbf{B_2}+ \mathbf{B_3})_z= (\alpha_1 + \alpha_2+ \alpha_3) \text{ at } z=0. \quad (19)$$

Since α_2 is zero, it will not always be shown explicitly. A mean global α_G values can be derived from a vector magnetogram define the sum of the α_i-values used in the special or general MDR method. Equation (19) is a result of assuming an equal distribution among the three constant-α component fields ($\mathbf{B_i}$, i=1,2,3). If the contributions are unequally weighted with ω_1, ω_2, and ω_3 then the equation is altered accordingly, i.e., ($\alpha_G = \omega_1\alpha_1 + \omega_2 \alpha_2+ \omega_3 \alpha_3$ with $\omega_1+ \omega_2 + \omega_3 = 1$).

The current helicity $\mathcal{H}_J$ is defined

$$\mathcal{H}_J = \int_V \mathbf{j}\cdot\mathbf{B}\ dV, \quad (19)$$

Hence for a volume V and from Equation (3), we have

$$\mathcal{H}_J = (\alpha_1+\alpha_2+\alpha_3)\ (1/\mu) \int_V |\mathbf{B}^2|\ dV. \quad (20)$$

Furthermore with the total energy defined by

E^T

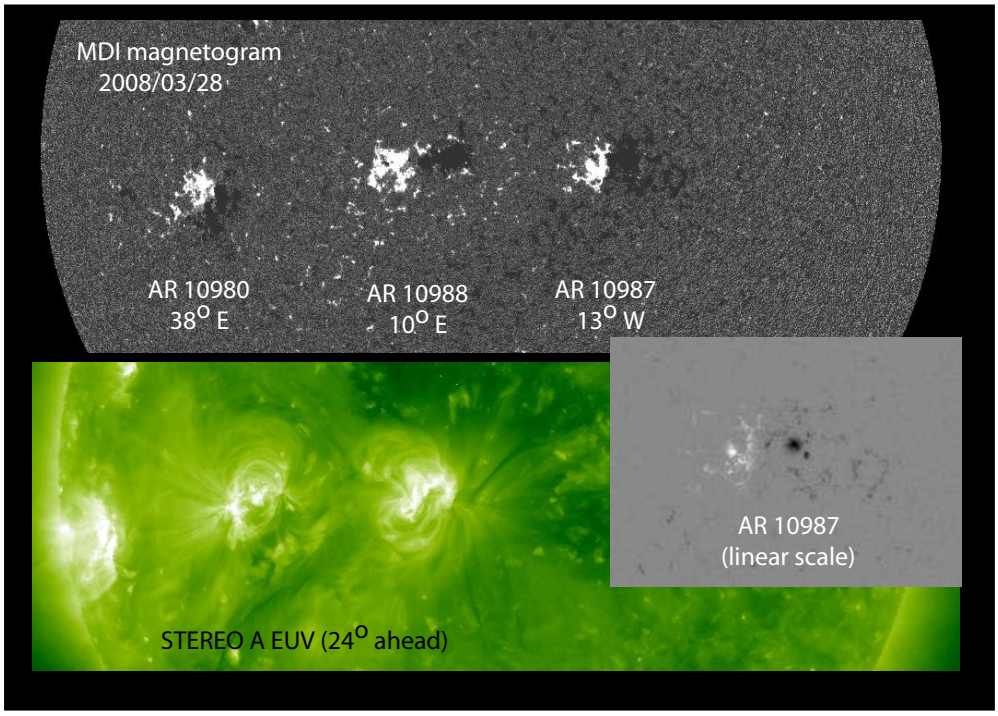

Figure 1. The MDI/SOHO and EUVI/STEREO data show the location for the AR 10987 (2008/03/08) on the solar disk. The insert with a linear scaling of the magnetic field shows that the active region is an average bipolar region.

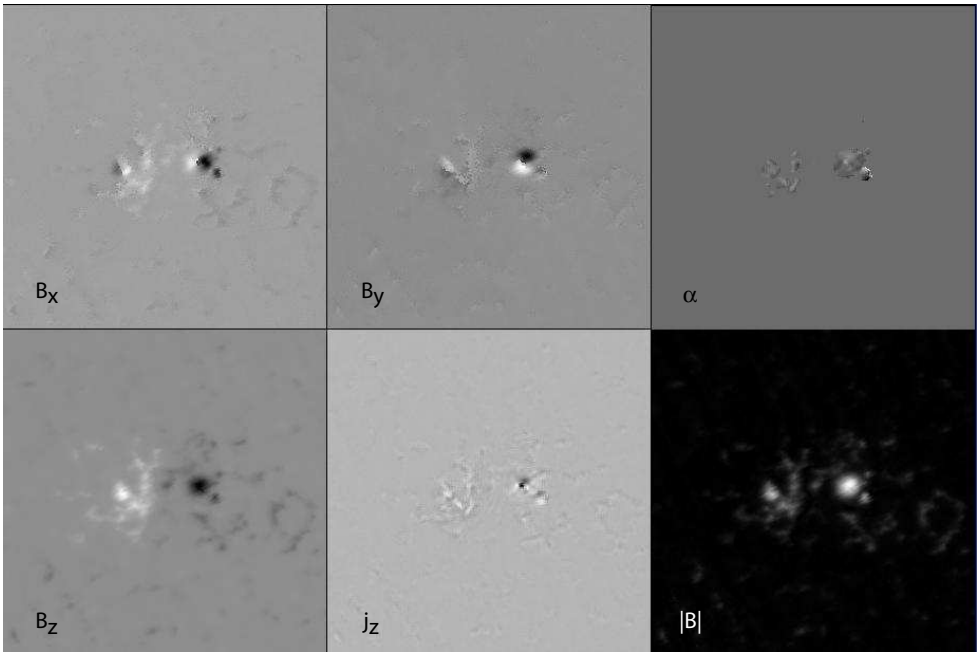

Figure 2. National Solar Observatory's SOLIS vector magnetogram data of AR 10987 is shown in the panels for the components of the magnetic field (B_x, B_y, B_z) and $|B|$, the electric current density (j_z), and the force-field parameter α. Only α values are calculated for $|B_z|>10$G and $|B_{transverse}|>100$G are assumed significant. In the upper right-hand panel, the α values outside of these restrictions have been set to zero. These panels illustrate the limited area of significant physical input that influences the coronal field models.

$$=(1/2\mu)\ \int_V\ |\mathbf{B^2}|\ dV \quad (21)$$

then by Schwarz inequality of Equation (24) we have

$$|\mathcal{H}_J| =\int_V\ |\mathbf{j\cdot B}|\ dV\ \le\ (2\mu/\eta)\ \mathbf{[}(\int_V\ \eta\,|\mathbf{j^2}|\ dV)\ ((1/2\mu)\int_V\ |\mathbf{B^2}|\ dV)\ \mathbf{]}^{1/2} \quad (22)$$

$$|\mathcal{H}_J| \le\ [2\mu/\eta\mathcal{R}\ E^T\ ]^{1/2} \quad (23)$$

Hence the Ohmic dissipation rate $\mathcal{R}$ for a given total magnetic E^T sets an upper bound on the current helicity. Equation (23) is given as a theoretical limit for the relevant MDR method, but are of limited practical interest. The most important physical quantity in a non-force-free magnetic field solution is the resulting Lorentz force density, which is discussed next.

Lorentz Force

Since a linear combination of constant-α force-free fields is not force free, we have non-zero Lorentz forces for the MDR field solutions. The value of the Lorentz force is given in this section. For the magnetic field **B** in Gauss and $\mu=4\pi$, the Lorentz force density in erg cm^{-3} is given as

$$\mathbf{L_F} = \mathbf{j}\ \mathrm{x}\ \mathbf{B} \quad (24)$$

$$\mathbf{L_F} = (1/\mu)\ (\alpha_1\ \mathbf{B_1} + \alpha_3\ \mathbf{B_3})\ \times (\ \mathbf{B_1} + \mathbf{B_2} + \mathbf{B_3}) \quad (25)$$

$$\mathbf{L_F} = (1/\mu)\{\alpha_1 \mathbf{B_1}\times\mathbf{B_2} + \alpha_1 \mathbf{B_1}\times\mathbf{B_3} + \alpha_3 \mathbf{B_3}\times\mathbf{B_1} + \alpha_3 \mathbf{B_3}\times\mathbf{B_2}\} \text{ (for } \alpha_2=0) \quad (26)$$

For $|\alpha_1|$ and $|\alpha_3|$ less than α_{max} $(=2\pi/L)$, then $|L_F| < |\alpha_{max}/\mu|\,|\mathbf{B_1}+\mathbf{B_3}|\,|\mathbf{B}|$, and for the case $|\mathbf{B_1}+\mathbf{B_3}|<|\mathbf{B}|$ then $|L_F| < |\alpha_{max/}\mu|\,B^2$, i.e. a small fraction of the magnetic energy pressure gradient. This inequality is expected when the potential field component $\mathbf{B_2}$ is the dominate component of the total field. L is the width of the magnetogram used in calculating the constant-α force-free fields. An estimate of the maximum pressure gradient is $d(B^2/8\pi)/dx \sim (\text{Max}|B(z=0)|)^2/D$, where D is the separation of the major magnetic concentrations. Assuming D~L/3 then

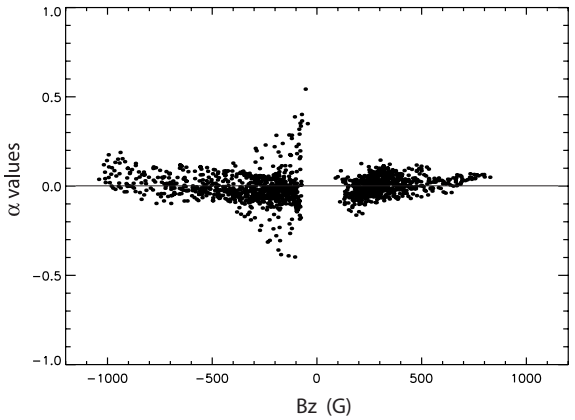

Figure 3. The local variation of the force-free field parameter α is derived from the SOLIS vector magnetogram data set. To avoid weak signal-to-noise values, the values of α calculated are limited to $|B_z|>10$ G and $B_{transverse}>100$ G. From these values the mean value is $\langle\alpha\rangle = -0.003$ and the standard deviation is 0.075, hence the data is consistent with a potential field (α=0).

$$L_F/[d(B^2/8\pi)/dx] < \alpha_{max}\, B^2/[B^2_{max}\, 3\alpha_{max}] \quad (27)$$

$$L_F/[d(B^2/8\pi)/dx] \leq B^2/B^2_{max}. \quad (28)$$

Typically the plasma pressure gradients and fluid force are needed to balance the Lorentz forces. For the data set described next, the resulting value of $L_F/[d(B^2/8\pi)/dx]$ versus height is given in Figure 6.

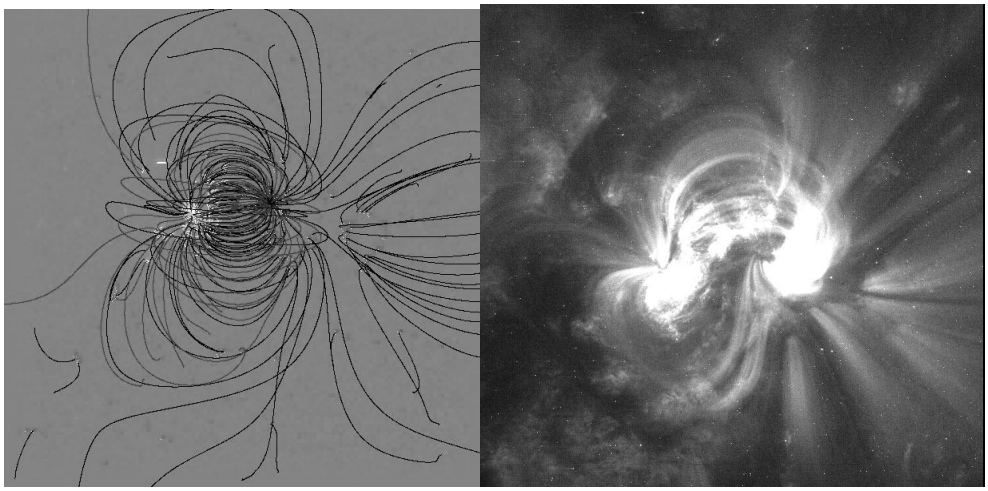

Figure 4. (a) The results of MRD field lines calculations for α=[0.02,0.,-0.02] show the field lines superimposed on a grey-scaled B_z image. From this perspective, the field lines are very similar to the potential field results. (b) The TRACE image for this region AR10987 is shown to the right.

Data Set

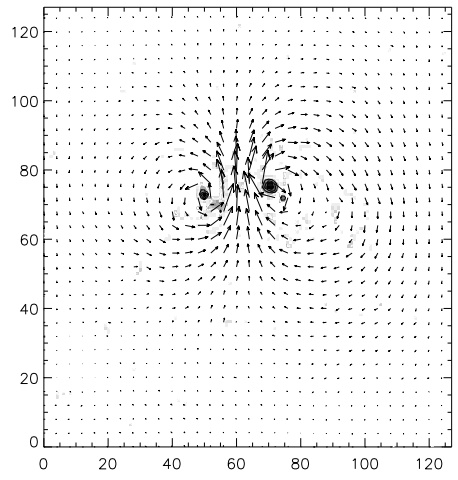

F

Figure 5. The vector field for MRD horizontal electric currents at the photosphere for α_1=0.02 shows that the electric currents are parallel to the surface for α_3= -α_1 and α_2=0. These currents inflate the magnetic field (cf., Figure 9). The vectors are shown on a gray scaled image of |B|.

Typical of the state of the observing technology, vector magnetograms of an active region show no consistent α value over the region yielding no definitive input into the MDR method. Only for extensively twisted active regions does a dominant set of α values emerge (cf. Gary 1995). The physical limit of calculating α is set by the generation of anomalous electric currents which are generated from seeing effects, polarimetric noise, imprecise de-ambiguitization, and spatial resolution, with larger errors in the umbra regions (Gary 1995). Even though the selected active region does not have a dominant twist, for our quantitative study, the active region AR10987 is used since it is a typical isolated, simple bipolar region. It allows a simple field configuration to be employed in the numerical studies. The physical setting of the region is given in Figure 1 showing the SOHO/MID data for the active region AR 10987 on 2008 February 28 and an EUV image from STEREO. The vector magnetogram data from the NSO/SOLIS archives is shown in Figure 2. This data allows the local variation of the force-free field parameter versus field strength derived from $\alpha = (\nabla\times\mathbf{B})_z/B_z$ (Figure 3). In Figure 3, the set of the noisiest α data has been eliminated and yet there is no trend for any specific alpha value. Because of this we need not attempt a numerical search for the best α-set using the minimum between the observed and calculated transverse differences. This data (Figure 3) confirms that there is no

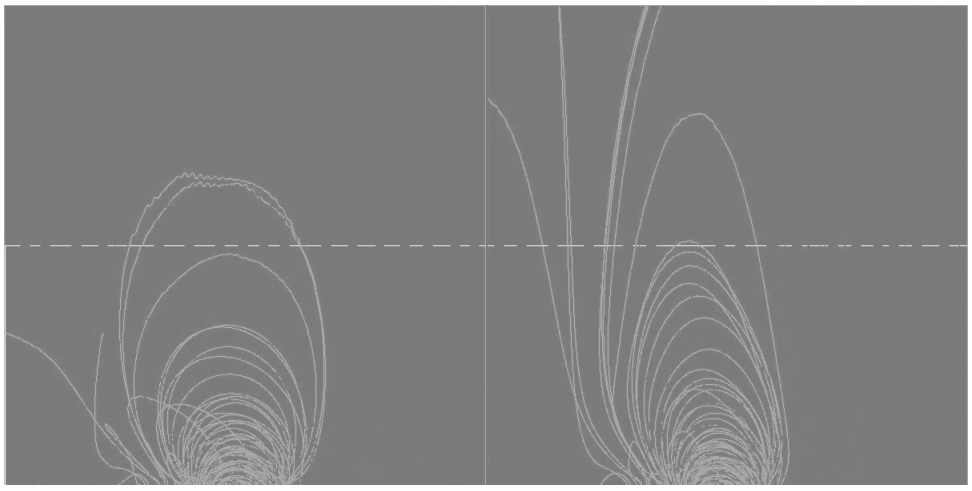

Figure 6. The field lines for two sets of α-values, {α_i}= [0,0,0] on the left (a), a potential solution, and {α_i} =[0.048,0.0,0.-048] on the right (b), show the inflation of the field lines as a result of the horizontal currents. A horizontal reference line is at half the box height.

significant twist to the region and the special α case, $\{\alpha_i\}=[\alpha_i,0, -\alpha_i]$, is consistent with the data (cf. Equation (19)). In the following we investigate this special α set (e.g., Figure 4).

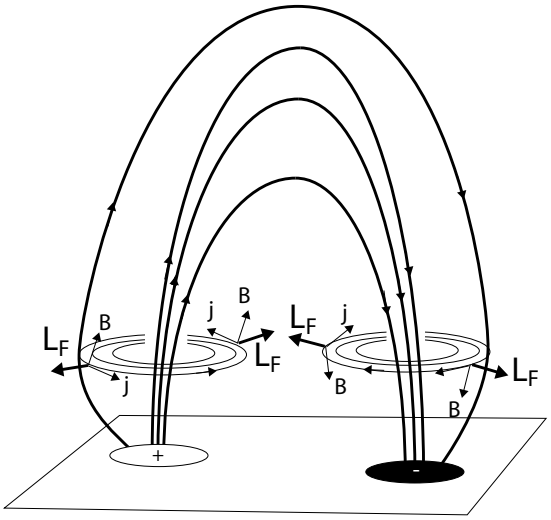

Figure 7. For AR 10987, this illustration shows the direction of the Lorentz force vectors for a set of electric currents generated by MDR field solution with a set α values of the form $[\alpha_i,0,-\alpha_i]$. For this case, the electric currents (two set of 3 thinner lines) circulate in a plane perpendicular to the photosphere. Explicit calculations show that there is a downward force above the magnetic inversion line.

Results

For the AR 10987 and using the MDR field solution, we have generated the magnetic field, electric currents, and Lorentz forces for selected cases of α sets $\{\alpha_i\} = [\alpha_i,0.,-\alpha_i]$ for $\alpha < \alpha_{max}=2\pi/L$, i.e. α values given unique solutions with finite energy (Gary 1989). Here L is the width of the magnetogram which can be in pixels or physical units depending on the use of the other spatial dimensions. Hu et al. (2008) describe the general method of the selection of the α sets employing both dual and single level magnetograms. Currently the use of magnetogram data makes this problematic, and we have averted this exercise in lieu of attempting to understand some of the physical consequences of the MDR method. Figure 4 shows the magnetic field lines for $\{\alpha_i\}=[0.02,0,-0,02]$ using the inverse pixel scale and with L=128, $\alpha_{max}=0.049$. The electric field density vectors at the photosphere (z=0) are shown in Figure 5, where there is no vertical component, $j_z=0$. These currents inflate the field. Using$\{\alpha_i\}= [0,0,0]$ and $\{\alpha_i\}= [0.048,0.0,0.-048]$, this inflation is seen in Figure 6 by comparing a set of field lines viewed perpendicular to the photosphere for each α set. The initial photospheric foot points are the same in each case. The inflation of the field is consistent with the observations made by Gary & Alexander (1999) in which the field lines of an inflated AR 7999 appeared to match the

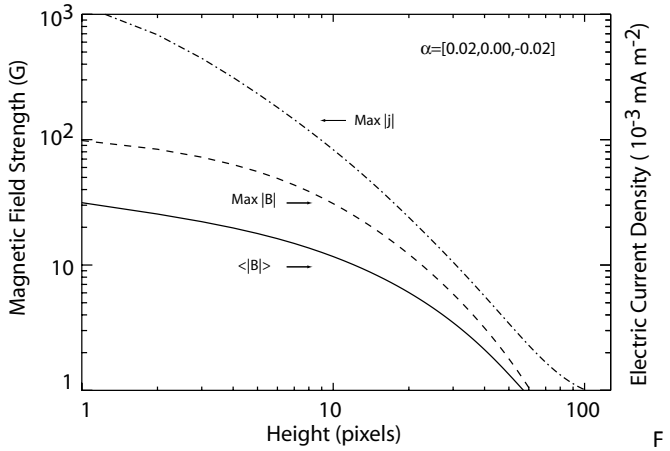

Figure 8. The variation of maximum |B| and average |B| is plotted versus height. The variation of maximum |j| versus height is scaled up by a factor of 10^3. Hence the maximum electric current density is 1 mA m^2, comparable with observed values.

Yohkoh/SXT observations. In their case the resulting Lorentz force is ~10^{-6} G^2/cm^4 resulting from the electric density of ~0.079 μA m^{-2}. In that study the horizontal electric currents were induced by radially stretching the magnetic field; in this study the horizontal currents generate an inflated field. As illustrated in Figure 7, the resulting Lorentz forces squeeze the plasma above the magnetic inversion line by opposite directed forces.

Using $\{\alpha_i\}$=[0.02,0,-0,02] in Figure 8, we show the height variation of the maximum and average magnetic field strength |B| and the maximum current density |j|. The calculations were performed for a 128×128×128 cube with a pixel unit equivalent to 2" (or 1450km) using numerically fast Fourier transform solutions of the three constant-α force-free-field components. Here $|\alpha_1|$ and $|\alpha_3|$ have been selected to have their values approximately half of maximum allowable for finite energy solutions, and hence are representative solutions the resulting Lorentz forces. The maximum |j| at the photosphere is ~2 mA m^{-2} which is an order of magnitude smaller than the maximum of the normal component j_z seen in typical solar active regions (Gary & Démoulin 1995). This infers that the electric currents are not unphysical and are consistent with observations.

Using the same α set, we show in Figure 9 the height variation of the maximum and average Lorentz forces per unit volume. The maximum Lorentz force per unit volume is 10^{-5} erg cm^{-4}. The other curves show these values normalized to the square of the magnetic field and are in units of inverse pixel length. For comparison the vertical magnetic pressure gradient is plotted showing that the Lorentz force is an order of magnitude higher at the surface and this difference

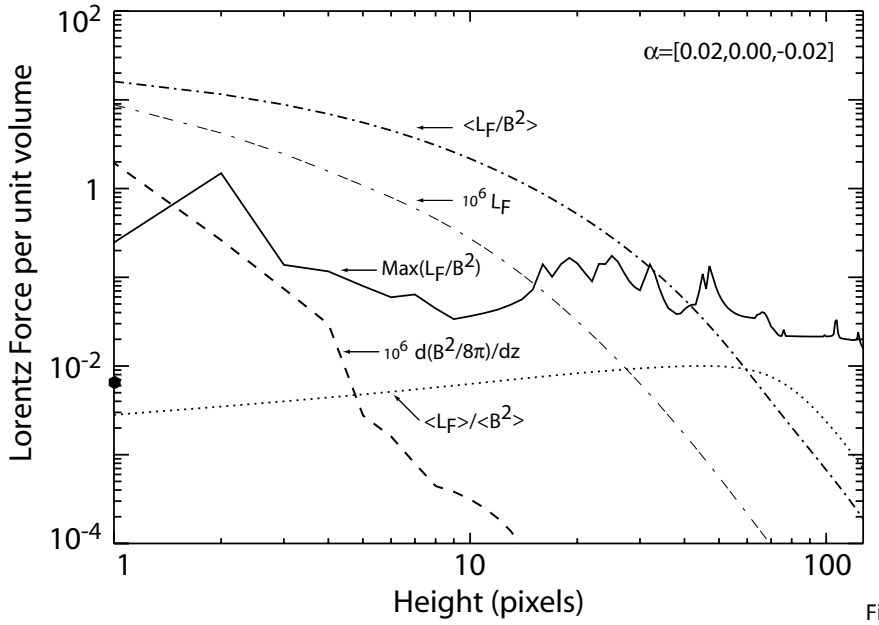

Figure 9. The variation of the maximum (max) and average (<>) values of the Lorentz force L_F is plotted vs. height. Various normalizations of the values by the square of the magnetic field are shown along with the vertical magnetic pressure gradient. These results are for an α set of α = 0.02,0.,-0.02]; however if $\alpha_1 \neq \alpha_3$, i.e., α= [0.02,0.,-0.01], the resulting values are similar, with L_F becoming slightly smaller, due to the electric field being more aligned with the magnetic field. Hence the case shown is an upper limit for $|\alpha_1| > |\alpha_3|$.

increases exponentially with height. Near the surface, the gravitational force per unit volume is shown on the ordinate as a solid circle at a value of 7.9×10^{-9} ergs cm^{-4} but is scaled to match the inflated (10^6) scales of L_F and $d(B^2/8\pi)/dz$. This indicates that both the magnetic pressure gradient force and the gravitational force are too small to counter the Lorentz force; hence pressure and fluid forces must be introduced to produce a stable plasma. How this is implemented physically is yet to be detailed in the MDR approach. The Lorentz force directions are illustrated in Figure 7. This shows the Lorentz force being outward from the central coronal arch connecting the two main (opposite) magnetic concentrations (umbrae) of the active region. This infers that the forces between the main magnetic concentrations would push the plasma together resulting in an increased pressure over the magnetic inversion line. This could then inflate the field further. The weaker force exterior to the magnetic concentrations would result in some unspecified external force, such as plasma pressure directed inward toward the active region.

Conclusion

We have evaluated the MDR method for deriving a coronal non-force free magnetic field solution and examined the particular case of the solutions where the other two α's are equal but of opposite signs. This special case is consistent with the observations of active region AR 10987 where local α values evaluated by $(\nabla \times B)_z/B_z$ over the region are consistent with a zero net twist. For the special case of $\{\alpha_i\} = [\alpha_i, 0., -\alpha_i]$, the resulting magnetic field is a vertically inflated magnetic field resulting from the electric currents being parallel to the photosphere. If the electric currents (as seen in Figure 7) inflate active region fields in general then these currents could be responsible for producing a north-south asymmetry in the observed helicity, however, this effect would be solar cycle dependent which it is not (Pevtsov 2008). Therefore, the only direct effect of an inflated field is the result of Gary and Alexander (1999). The Lorentz force is a factor of ten higher than the magnetic force component, $d(B^2/8\pi)/dz$. Most of the force is countered by an opposite directed force on either side of the magnetic inversion line. This could lead to an increased pressure above the inversion line and further inflate the field. The calculated photospheric electric current densities are an order smaller than the maximum observed in active regions in general. Hence the electric currents and Lorentz forces generated seem not to be unrealistic with respect to possible solar dynamics. We concur with the comments made by DeRosa et al. (2008) in that without improved and additional plasma data, we advise that the implementation of this or any other extrapolation using the electric current density as a lower boundary condition must be done cautiously. The MDR method is more appropriate for theoretical investigations rather than analysis of the magnetic field configurations for active regions. However, this study of the special α-case infers that a general inflation of the magnetic field could be consistent with the observations.

I am grateful to Q. Hu, R. Moore, S. Suess, and S. T. Wu for useful discussions. I would like to acknowledge A. Norton at the National Solar Observatory for her assistance in preparing the SOLIS vector magnetograms for this research.

References

Bhattacharyya, R., and Janaki, M. S.: 2004, Physics of Plasmas, 11, 5615.

Bhattacharyya, R., Janaki, M. S., Dasgupta, B, and Zank, G. P.: 2007, Solar Phys., 240, 63.

Chandrasekhar, S., and Woltjer, L.: 1958, Proc. National Acad. Sci., 44, 285.

Dasgupta, B., Dasgupta, P., Janaki, M. S., Watanabe, T., and Sato, T.: 1998, Phys. Rev. Letters , 81, 3144.

Dasgupta, B., Shaikh, D., Hu, Q., and Zank, G. P.: 2008, J. Plasma Phys., pub. Online 8 Oct 2008.

DeRosa, M.L., Carolus J. Schrijver, C. J., Barnes, G., Leka, K. D., Lites, B. W., Aschwanden, M. J., Amarim, T., Canou, A., McTiernan, J. M., Régnier, S., Thalmann, J. K., Valori, G., Wheatland, M. S., Wiegelmann, T., Cheung, M. C. M., Conlon, P. A., Fuhrmann, M., Inhester, B., and Tadesse, T.: 2008, Ap. J. (submitted).

Hu, Q., Dasgupta, B., Choudhary, D. P., and Buchner, J.: 2008, Ap. J., 679,848.

Hu, Q., and Dasgupta, B.: 2008, Solar Phys., 247, 87.

Gary, G. A.: 1989, Ap. J. Suppl., 69, 323.

Gary, G. A., and Démoulin, P.: 1995, Ap. J., 445, 982.

Gary, G. A., and Alexander, D.: 1999, Solar Phys., 186, 123.

Gary, G. A.: 2001, Solar Phys., 2003, 71.

Golub, L., and Pasachoff, J. M.: 1997, *The Solar Corona*, Cambridge University Press, Cambridge, UK.

Pevtsov, A. A.: 2008, Astron. Astr., 29, 49.

Taylor, J. B.: 1974, Phys. Rev. Letters, 33, 1139.

Woltjer, L.: 1958, Proc. National Acad. Sci., 44, 489.

Appendix A. Ohmic Heating in Parallel Resistor Circuit

The following is a simple example using the minimum dissipation rate assumption to derive information about a physical system (see Figure A1). It assumes that the irreversible process of energy loss from electric resistivity is characterized by the minimum value of the entropy production, the total Ohmic heating loss rate. For an electric circuit with two parallel resistors R_1 and R_2 and the associated currents I_1 and I_2, the Ohmic heating is given by

$$E = I_1^2 R_1 + I_2^2 R_2 \text{ or } E = I_1^2 R_1 + (I-I_1)^2 R_2 , \quad \text{(A1)}$$

where I is the total current in the circuit. The minimum Ohmic heating rate is obtained at the extrema when the current in the two resistors is varied, i.e., at the point given by

$$dE/dI_1 = 2\, I_1 (R_1 + R_2) - 2\, I\, R_2 = 0 \quad (A2)$$

Hence the minimum dissipation rate gives the distribution of the currents:

$$I_1 = I / (R_1/R_2 + 1), \quad (A3)$$

$$I_2 = I/(R_2/R_1 + 1). \quad (A4)$$

Note that the minimum heating rate given by Equation (A2) gives the voltage across the resistors as per Ohm's Law, i.e., Equation (A2) gives,

$$2\, I_1 (R_1 + R_2) = 2\, (I_1 + I_2)\, R_2$$

or

$$I_1 R_1 = I_2 R_2.$$

Hence the minimum dissipation rate in this electric circuit is consistent with the Ohm's laws.

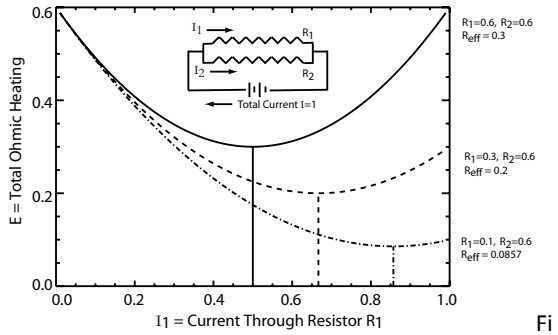

Figure A1. The total Ohmic heating rate (E) is plotted as a function of the electric current I_1 through resistor R_1 for a set of two parallel resistor values (R_1, R_2). The minimum values are given by Equation A2 and since the total current is I=1, the heating rate is numerically equal to the effective resistance (R_{eff}) of the parallel resistor circuit.

Appendix B. Variational Solutions for Magnetic Fields Solutions

From a variational of the total energy given a constant global magnetic helicity,

$$\delta W = \delta[\ (1/2\mu) \int_V \mathbf{B}^2\, dV - \varepsilon \int_V \mathbf{A}\cdot\mathbf{B}\, dV\ ] = 0, \quad \text{[MKS units]} \quad (B1)$$

Woltjer (1958) derived, for a closed system, the linear force-field equation:

$$\nabla\times\mathbf{B} = \alpha\mathbf{B}. \quad (B2)$$

From a variational of the total magnetic energy given a constant global mean-square current density,

$$\delta W = \delta[\ (1/2\mu) \int_V \mathbf{B}^2\, dV - \varepsilon \int_V \eta\, \mathbf{j}^2\, dV\ ] = 0, \quad (B3)$$

Chandrasekar &Woltjer (1958) , for a closed system, derived the magnetic field equation,

$$\nabla\times\nabla\times\mathbf{B} = \alpha^2\mathbf{B}. \quad (B4)$$

In a similar manner, but for an open system, using the variational of the constant Ohmic dissipation rate given constant relative magnetic helicity,

$$\delta W = \delta[\ \int_V \eta\, \mathbf{j}^2\, dV - \varepsilon' \int_V (\mathbf{A}+\mathbf{A}_p)\cdot(\mathbf{B}-\mathbf{B}_p)\, dV] = 0, \quad (B5)$$

we can derive the field equation

$$\nabla\times\nabla\times\nabla\times\mathbf{B} = \alpha\mathbf{B}, \quad (B6)$$

which is the same as Equation (1).

The proof of Equation (B5) is as follows. Starting with Equation (B5) and substituting $\mu\,\mathbf{j} = \nabla\times\mathbf{B}$, we have

$$\delta w = \delta[\int_V (\eta/\mu^2)\,(\nabla\times\mathbf{B})^2\,dV - \varepsilon'\int_V (\mathbf{A}+\mathbf{A}_p)\cdot(\mathbf{B}-\mathbf{B}_p)\,dV]] = 0 \qquad (B7)$$

$$(\mu^2/\eta)\,\delta w = \int_V [2\,(\nabla\times\mathbf{B})\cdot(\nabla\times\delta\mathbf{B}) - \varepsilon\,\delta(\mathbf{A}+\mathbf{A}_p)\cdot(\mathbf{B}-\mathbf{B}_p) - \varepsilon\,(\mathbf{A}+\mathbf{A}_p)\cdot\delta(\mathbf{B}-\mathbf{B}_p)\,]\,dV = 0 \quad (B8)$$

where $\varepsilon' = \varepsilon\eta/\mu^2$. Now using the triple scalar product in the form $\mathbf{a}\cdot(\nabla\times\mathbf{b}) = \mathbf{b}\cdot(\nabla\times\mathbf{a}) - \nabla\cdot(\mathbf{a}\times\mathbf{b})$, we have the following,

$$2\,(\nabla\times\mathbf{B})\cdot(\nabla\times\delta\mathbf{B}) = 2\,\delta\mathbf{B}\cdot(\nabla\times\nabla\times\mathbf{B}) - 2\,\nabla\cdot[(\nabla\times\mathbf{B})\times\delta\mathbf{B}] \qquad (B9)$$

and

$$\varepsilon\delta(\mathbf{A}+\mathbf{A}_p)\bullet(\nabla\times\mathbf{A}-\nabla\times\mathbf{A}_p)+\varepsilon(\mathbf{A}+\mathbf{A}_p)\bullet\,\delta\,(\nabla\times\mathbf{A}-\nabla\times\mathbf{A}_p) =$$

$$\varepsilon(\delta\mathbf{A})\bullet((\nabla\times\mathbf{A})-(\nabla\times\mathbf{A}_p)) + \varepsilon\,\delta\,\mathbf{A}\bullet(\nabla\times(\mathbf{A}+\mathbf{A}_p)) - \varepsilon\,\nabla\bullet((\mathbf{A}+\mathbf{A}_p)\times\delta\,\mathbf{A}) . \qquad (B10)$$

Substitution yields the following for the bracket term [ ] of Equation (B8):

$$2(\nabla\times\mathbf{B})\bullet(\nabla\times\delta\mathbf{B})+\varepsilon\,\delta(\mathbf{A}+\mathbf{A}_p)\bullet(\mathbf{B}-\mathbf{B}_p) + \varepsilon(\mathbf{A}+\mathbf{A}_p)\bullet\delta(\mathbf{B}-\mathbf{B}_p) =$$

$$2\delta\mathbf{A}\bullet(\nabla\times\nabla\times\nabla\times\mathbf{B}) - 2\nabla\bullet((\nabla\times\nabla\times\mathbf{B})\times\delta\mathbf{A} - 2\,\nabla\bullet[(\nabla\times\mathbf{B})\times\delta\mathbf{B}$$

$$+\varepsilon(\delta\mathbf{A})\bullet((\nabla\times\mathbf{A})-(\nabla\times\mathbf{A}_p)) + \varepsilon\,\delta\,\mathbf{A}\bullet(\nabla\times(\mathbf{A}+\mathbf{A}_p)) - \varepsilon\nabla\bullet((\mathbf{A}+\mathbf{A}_p)\,\delta\,\mathbf{A} \quad (B11)$$

The equation (B7) becomes

$$\delta w/\eta = \int 2(\nabla\times\mathbf{B})\bullet(\nabla\times\delta\mathbf{B})+\varepsilon\,\delta(\mathbf{A}+\mathbf{A}_p)\bullet(\mathbf{B}-\mathbf{B}_p) + \varepsilon(\mathbf{A}+\mathbf{A}_p)\bullet\delta(\mathbf{B}-\mathbf{B}_p)\,dv =$$

$$= \int \delta\mathbf{A}\bullet[2\,(\nabla\times\nabla\times\nabla\times\mathbf{B}) + \varepsilon((\nabla\times\mathbf{A})-(\nabla\times\mathbf{A}_p))+\varepsilon\,(\nabla\times(\mathbf{A}+\mathbf{A}_p))\,]\,dv +$$

$$+\int\nabla\bullet[-2(\nabla\times\nabla\times\mathbf{B})\times\delta\mathbf{A} - 2[(\nabla\times\mathbf{B})\times\delta\,\mathbf{B} - \varepsilon\,((\mathbf{A}+\mathbf{A}_p)\times\delta\,\mathbf{A})\,]dv = 0 \qquad (B12)$$

The second integral, which can be written as a the following surface integral,

$$\int 2\,(\nabla\times\nabla\times\mathbf{B})\bullet(\,\mathbf{dn}_s\times\delta\mathbf{A}\,) + \int 2\,\delta\mathbf{B}\bullet(\,\mathbf{j}\times\mathbf{dn}_s\,) + \int\varepsilon\,(\mathbf{A}+\mathbf{A}_p)\bullet(\,\mathbf{dn}_s\times\delta\mathbf{A}\,)$$

is zero since it can be converted to a surface integral via Green's theorem and imposing the boundary conditions of Dasgupta et al.(1998) i.e., $\delta\mathbf{A}\times\mathbf{dn}_s=0$ **and** $\mathbf{j}\times\mathbf{dn}_s=0$. The integrand in the first integral must be zero since in the volume $\delta\mathbf{A}$ is arbitrary, hence

$$(\nabla\times\nabla\times\nabla\times\mathbf{B}) = \varepsilon\,\mathbf{B}. \qquad (B13)$$

Appendix C. Discussion of Units

The force-free-field parameter α is expressed in the unit of inverse length (L^{-1}) giving the value of $\alpha\mathbf{B} = (\nabla\times\mathbf{B})$ in units of G cm^{-1}. The relation to current density ($j=\alpha B/\mu$) is given by the conversion relation 1 G cm^{-1} = 1.2×10^{-4} A cm^{-2}. If the pixel units are Δx= 1 arcsec then $\Delta x=0.725\times10^{8}$ cm and if $\alpha=0.01$ in units of inverse pixels, then $\alpha=0.01/0.725\times10^{8}$ cm^{-1} = 0.0138×10^{-8} cm^{-1}. Gary (1987) gives maximum of the force-free field parameter for fields of finite energy as $\alpha_{max}=2\pi/128=0.049$ in pixel units for an array size of 128 pixels. Hence, for a value of $\alpha=0.01$ $pixel^{-1}$ value and for an electric current density j = (0.0138×10^{-8} cm^{-1})(100G)(1.2×10^{-4} A cm^{-2}/G cm^{-1})= 1.66×10^{-12} A cm^{-2} = 1.66×10^{-8} A m^{-2} , the Lorentz force is L_f= j αB = (0.0138×10^{-8} cm^{-1})$(100G)^2$= 1.38×10^{-4} G^2 cm^{-1}= 1.38×10^{-4} erg cm^{-3} given that j is perpendicular to B. The ratio of L^f/E_M =

1.38×10^{-4} / 3.99×10^{-4} =0.346, where the E_M magnetic density is $E_M=B^2/8\pi$ ergs cm^{-3} for B in Gauss.